

# Spectral Properties of HEMA/poly(HEMA) as Ligand in Luminescent Europium Based Complexes Through Computational Investigation

ELENA SIMONA BACAITA<sup>1\*</sup>, CORNELIU SERGIU STAN<sup>2</sup>, MARICEL AGOP<sup>1,3</sup>, GABRIELA CIOCA<sup>4\*</sup>

<sup>1</sup> Gheorghe Asachi Technical University of Iasi, Faculty of Machine Manufacturing and Industrial Management, Department of Physics, D. Mangeron 73 Ave, 700050, Iasi, Romania

<sup>2</sup> Gheorghe Asachi Technical University of Iasi, Faculty of Chemical Engineering and Environmental Protection, Department of Natural and Synthetic Polymers, Gheorghe Asachi D. Mangeron 73 Ave, 700050, Iasi, Romania

<sup>3</sup> Acad Romanian Scientists, 54 Splaiul Independentei, Bucharest 050094, Romania

<sup>4</sup> Lucian Blaga University of Sibiu, Preclinical Department, Faculty of Medicine, Victoriei Bld. No. 10, Sibiu, 550024, Romania

*This paper investigates, through computational methods, the spectral properties of (2-hydroxy ethyl) methacrylate used as ligand in a luminescent complex based on europium, aiming to show that the absorption spectra is determined by the ligand type and the emission spectra is specific for each lanthanide.*

*Keywords: luminescent, spectral, HEMA, europium*

Lanthanide complexes have been intensively studied in the last decade due to their high potential for different applications in cancer diagnosis and therapy, as cytotoxic agents and inhibitors, in photodynamic therapy, radiation therapy, drug/gene delivery, biosensing, and bioimaging [1-3]. Since 1985 when FDA approved the clinical use of the magnetic resonance imaging (MRI), this non-invasive diagnostic method has become extensively used in all medical fields. The MRI contrast agents, such as gadolinium ion (Gd<sup>3+</sup>) complexes, or superparamagnetic ironoxide (SPIO) nanoparticles (NPs), are a unique class of pharmaceuticals that are used to enhance the image contrast between normal and diseased tissue and indicate the status of organ function or blood flow after intravascular (iv) administration, increasing the accuracy of diagnosis, but doesn't offer a real-time, highly sensitive, and selective biochemical information [4, 5]. In this context, the combination of MRI and fluorescence imaging (FI), as a dual imaging application, should provide a balance between iconography and histology and then the diagnosis and treatment are likely to be more accurate and sensitive. With this approach, tumors are positioned with MRI and completely removed under the guidance of FI [6, 7]. A limitation of this possibility is that each imaging modality uses different contrasting agents with distinct chemical compositions and pharmacological properties.

Lanthanide ions are ideal luminescent probes for biological systems [8] because of their narrow emission bands, easily recognizable and, even more, there are known to have bacteriological effects, property that may be considered an advantage in curing diseases, including cancer [9-11]. In order to benefit of their properties lanthanide ions had to be inserted into highly stable macromolecular structures. This was done taking into consideration one lanthanide ion property: they bind preferentially to highly electronegative elements, present as ligating atoms of polyatomic molecules (*ligands*) [12, 13].

Under UV irradiation, the ligand absorbs a UV photon and this gain in energy causes one electron of the ligand to make the transition from the ground singlet state to the first excited singlet state; in this state, the electron has the same spin as in the original ground state, i.e. opposite to that of the other member of the pair in the ground state.

From this excited state of the ligand, three return paths to the ground state are possible:

i) the direct reverse transition from the first excited singlet state to the ground singlet state by radiative emission: the phenomenon of *fluorescence*;

ii) if one excited triplet state is available, intersystem crossing may occur, i.e. the electron changes its spin orientation and the ligand passes from the excited singlet to the excited triplet state with radiationless emission of a small amount of energy, from where it can decay to the original ground singlet state, again with a change in electron spin orientation; the last transition is a radiative emission: the phenomenon of *phosphorescence*;

iii) if the ligand is bound to a lanthanide ion, the electron from the excited triplet state of the ligand *crosses* to the lanthanide ion, resulting in the promotion of its 4f electrons to an excited state; finally, the lanthanide ion returns to its ground states by radiative emission: the phenomenon of *luminescence*. This mechanism is also known as ligand-to-metal charge-transfer (LMCT) mechanism and is seen as a shift of charge density between molecular orbitals (MO) of ligand and metal [14].

The energy transfer pathway described above is illustrated in figure 1.

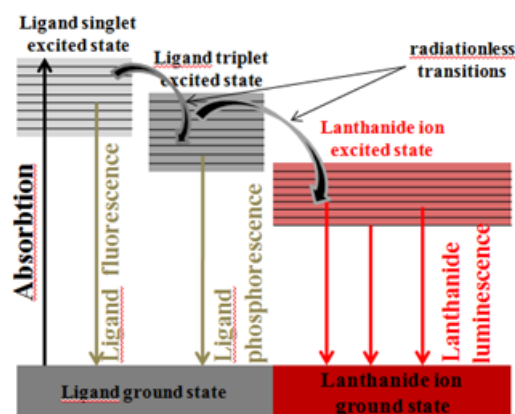


Fig. 1. Energy transfer process involved in the luminescence of Eu<sup>3+</sup> complexes of organic ligands

\* email: [bacaita@tuiasi.ro](mailto:bacaita@tuiasi.ro); [gabriela.cioca@ulbsibiu.ro](mailto:gabriela.cioca@ulbsibiu.ro)

This mechanism explains two important characteristics of lanthanide complexes: i) the absorption /excitation spectra are broad and fairly similar for all lanthanide complexes with the same ligand because they are determined by ligand transitions from the the ground to its excited electronic states that consists of many closely spaced vibrational levels; ii) the emission spectra are sharp because they involve transitions of the lanthanide ion electrons from higher excited level to lower 4f energy levels, characteristic of each ion  $\text{Ln}^{3+}$ , depending on electronic configuration of each ion. Also, these intersystem crossing steps provide a simple explanation for the long lifetimes, up to 2 ms, observed for the luminescence of  $\text{Ln}^{3+}$  complexes.

Parker and Williams [15] have stated a very simple and comprehensive description for the luminescence mechanism of lanthanide complexes: ligands behave like an *antenna* which absorbs strongly at a suitable wavelength and transfers its excitation energy to the lanthanide ion which, on accepting this energy, becomes excited to the emissive state, and emits energy when passing to the ground state.

In this paper our attention is focused on a new polymer complex -Poly(EuHEMA) - based on poly(2-hydroxy ethyl) methacrylate (P-HEMA) and europium (Eu) as transition metal, well known for its intense red photoluminescence.

In this compound, the lanthanide acts as a trivalent ion,  $\text{Eu}^{3+}$ , with 60 electrons in the configuration  $[\text{Xe}]4f^6$ ; the six electrons in the 4f shell can be arranged in 3003 different ways into the seven 4f orbitals, each one defining a different energetic state of the ion; so, the total degeneracy of  $\text{Eu}^{3+}$  is 3003. Each state is noted as  $^iL_J$ , where i) L is the total orbital angular momentum quantum number, usually replaced with the corresponding capital letter, ii) S is the spin multiplicity (a number that gives information on the number of unpaired electrons) and iii) J the total angular quantum number ( $J \in [L+S, |L-S|]$ ). For the  $\text{Eu}^{3+}$ , with 4f<sup>6</sup> configuration, the following states are possible: i) L can be 0, 1, 2, 3, with the corresponding states denoted with S, P, D, F; ii) singlets (S=1 - all electrons are paired), triplets (S=3 - two electrons unpaired), quintets (S=5 - four unpaired electrons) and septets (S=7 - six unpaired electrons); iii) J can be 6, 5, 4, 3, 2, 1, 0. Based on Hund's rules, it was established that, for  $\text{Eu}^{3+}$ ,  $^7F_0$  is the ground state and, therefore, the order of energies for the other 4f levels is  $^7F_0 < ^7F_1 < ^7F_2 < \dots < ^7F_6$ . However, the positions of the excited states can be determined only by calculations [16].

If for  $\text{Eu}^{3+}$ , information on the electronic configuration could easily be obtained using the existing theories, getting, in a theoretical approach, this information for complex molecules (such as HEMA or polyHEMA).. is quite challenging, even for theoreticians, since it implies solving the Schrodinger equation for large molecules and applying molecular orbital theory for the determination of the wave function and the energy of a quantum many-body system [17]; plus, in general, the relativistic effects are more important for heavier the lanthanide atom.

As an alternative to the existing theories, the computational approach was proved to be able to offer additional information on the lanthanide complexes structures and properties. One way is the use of semiempirical Sparkle model (AM1 [18], PM3 [19], PM7 methods), further implemented in the LUMPAC software, efficient and user-friendly software, able to carry out, with low computational effort, analysis of luminescence of lanthanide containing systems [20], with reasonable accuracy. Still, despite this, semiempirical methods suffer

from the general problem of dependence on the parametrization procedure and, in the specific case of lanthanides, from the lack of metal ion-ligand atom core interactions, which are only partially taken into account by the pseudocenter approach.

Density Functional Theory (DFT) calculations overcomes this shortcoming: they offer higher accuracy in the calculation of the ground state geometry of the lanthanide complexes, of crucial importance for the quality of spectroscopic properties prediction, but with the disadvantage of high time-consuming procedures [21].

An advantage in using DFT methods to lanthanide complexes is that they have also implemented time-dependent density functional theory (TD-DFT) through which the excited states of molecules can be calculated, allowing thus the determination of theoretical absorbance/emission spectra.

In this paper, we aim to study the spectral properties of HEMA/poly(HEMA) through the computational methods described above with emphasis on the calculation of the excited states of the ligand structures on which the lanthanide complex is based on.

## Experimental part

Luminescent polymer complexes based on poly(2-hydroxy ethyl) methacrylate (P-HEMA) and  $\text{Eu}^{3+}$  were prepared (for details, see [22]). XPS and FT-IT investigations revealed that the lanthanide ion bonds to the HEMA structure by: (1) a covalent bond with the oxygen atom in the hydroxyl group located on the side of the HEMA monomer chain and (2) a coordinative bond with the oxygen atom in the carbonyl group. Moreover, they showed the presence of three water molecules in the first coordination sphere, but with very little effect on luminescence, since the lanthanide complex is achieved in solid crystalline form. As consequence, the proposed structure of the complex, before photopolymerization, is illustrated in figure 2.

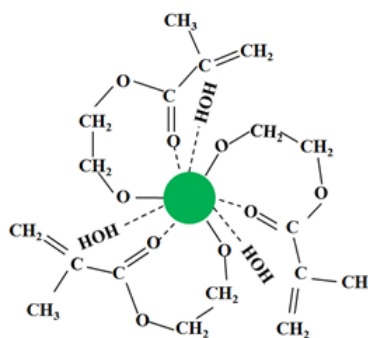


Fig. 2. The proposed structure of  $\text{Eu}^{3+}$  complex

The fluorescence analysis showed absorption peaks at 332-334 nm, while emission peaks were at 590 nm and 614 nm, identified as corresponding to the  $^5D_0 \rightarrow ^7F_1$  and  $^5D_0 \rightarrow ^7F_2$  transition of the lanthanide ion  $\text{Eu}^{3+}$ , being known the energies of these levels:  $^5D_0$  (17.227  $\text{cm}^{-1}$ ),  $^7F_1$  (379  $\text{cm}^{-1}$ ),  $^7F_2$  (1043  $\text{cm}^{-1}$ ).

The excitation/emission spectra of this complex are presented in figure 3.

## Computational procedure

The computational procedure follows the next steps:

(1) The initial model structure of HEMA was built with Avogadro program [23]. The resulting structure was used as input in Gaussian 09 [24] for optimizing its geometry through B3LYP method at 6-311+G(d,p) level;

(2) The optimized structure of HEMA was imported in Amber16 [25] to generate prep input files for the terminal residues (head - HEM and tail - EMA) and the middle residue (MEM) of the poly(HEMA), using *prepgen* command

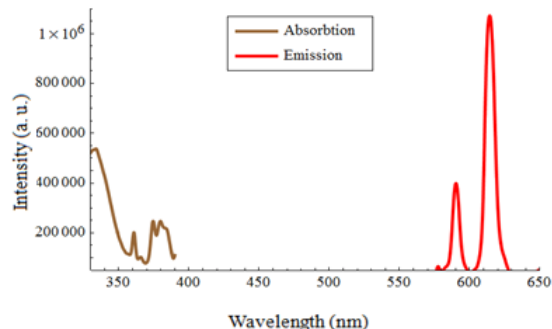


Fig. 3. Absorption and emission spectra of luminescent complex based on  $\text{Eu}^{3+}$

available in AmberTools; with these three prep files, the structure of polymers with different polymerization degree (DP) can be created in xleap, with *sequence* command. In this study, we created a polymer with DP=3, since the luminescent polymer complexes were prepared at 1:3 metal to ligand ratio;

(3) The structure previously obtained was submitted to a minimization of energy in Amber16 in order to find the

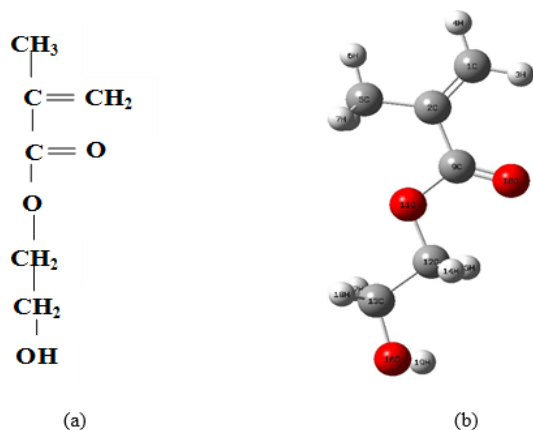


Fig. 4. The structure of HEMA monomer: schematic (a), optimized (b)

most stable state of the polymer; minimization were performed in vacuum, without periodic boundary conditions, at 300 K, for 100 ps, with *gaff* Amber force field;

(4) The stabilized poly(HEMA) structure was used in the calculation of the singlet excited states with TD-DFT method, B3LYP/ 6-31+G(d,p) level., in Gaussian 09;

(5) From the analysis of the Gaussian output file, the absorption spectra were plotted.

## Results and discussions

### Electrostatic characterization of HEMA and poly(HEMA) in electrically neutral state

The structure of the HEMA monomer is shown in figure 4 and the calculated partial atomic charges are listed in table 1.

The structure of the poly(HEMA) with DP=3 is shown in figure 5 and the calculated partial atomic charges are listed in table 1.

Analyzing the above values, one observation is that the highest difference, between the charge of an atom in monomer and the charge of the same atom (equivalent atom) in polymer configuration, is for the carbon atoms

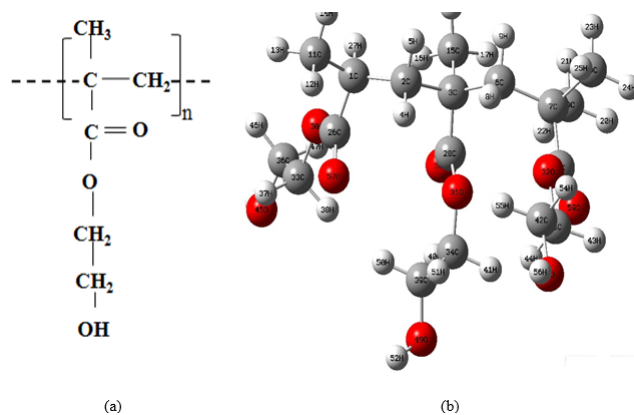


Fig. 5. The structure of poly(HEMA): schematic (a), optimized for DP=3 (b)

Nume atom (HEMA)	Sarcina atom	Atomi echivalenți (polyHEMA: HEM, MEM, EMA)	HEM (unități sarcină atomică:e)	MEM (unități sarcină atomică:e)	EMA (unități sarcină atomică:e)
1C	-0.274	2C, 6C, 19C	-0.1356	-0.4364	-0.4326
2C	0.032	1C, 3C, 7C	0.0833	0.3135	0.4251
3H	0.103	4H, 8H, 20H	0.0271	0.0768	0.0980
4H	0.127	5H, 9H, 21H	0.0504	0.1081	0.1070
5C	-0.399	11C, 15C, 10C	-0.4600	-0.4163	-0.4685
6H	0.133	12H, 17H, 23H	0.1161	0.1034	0.1161
7H	0.106	13H, 16H, 24H	0.1144	0.0819	0.1090
8H	0.105	14H, 18H, 25H	0.1258	0.0930	0.1108
9C	0.602	26C, 28C, 29C	0.9361	0.7041	0.7791
10O	-0.393	57O, 58O, 59O	-0.6468	-0.5561	-0.6012
11O	-0.37	30O, 31O, 32O	-0.6787	-0.5083	-0.5769
12C	0.068	33C, 34C, 35C	0.4401	0.1316	0.3709
13C	0.13	36C, 39C, 42C	0.1869	0.2338	0.2109
14H	0.063	37H, 40H, 43H	0.0143	0.0861	0.0201
15H	0.052	38H, 41H, 44H	0.0150	0.0940	0.0320
16O	-0.462	45O, 49O, 53O	-0.7346	-0.7035	-0.7247
17H	0.025	46H, 50H, 54H	0.0220	0.0338	0.0092
18H	0.052	47H, 51H, 55H	0.0230	0.0130	0.0131
19H	0.298	48H, 52H, 56H	0.4444	0.4241	0.4384

**Table 1**  
CALCULATED PARTIAL ATOMIC CHARGES OF HEMA AND POLY(HEMA) ATOMS

from the main chain (equivalent to 1C, 2C) and for the oxygen atoms (equivalent to 10O, 11O, 16O); this can lead to the idea that these atoms are the most subjected to electrostatic interactions.

Considering the quantum nature of the electron, we represented the molecular orbitals (fig. 6). The colors of the orbital lobes reflect the phases of the orbital (blue – positive phase, red – negative phase), with no physical meaning, but useful, in this case, to have an image on the orbitals of HEMA monomer residues (fig. 6a) and on the result of their overlapping when a supramolecular entity, poly(HEMA) with DP=3, is formed (fig. 6b).

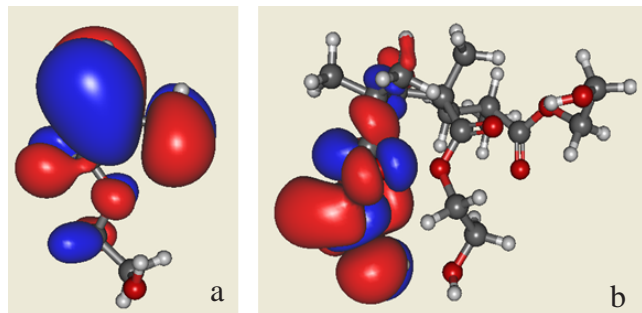


Fig. 6. The molecular orbitals of HEMA (a) and poly(HEMA) with DP=3 (b)

Knowing that the orbitals can be defined as the regions of space around the nucleus in which the probability of finding the electron has a maximum value, analyzing, by comparison, the figures 6a and 6b, the modification of electron density distribution can be observed: from the main chain to the branch chain and towards one terminal residue of the polymer, determining thus a weak affinity for chemical reactions for the atoms with no drawn orbitals. This indicates that in the complexation reaction [22], the bonding appears between the lanthanide ion and the oxygen atoms of one terminal residuu.

#### Spectral properties of HEMA and poly(HEMA) in electrically neutral state

Excited state calculations were performed for HEMA and poly(HEMA) for the determination of the absorption spectra.

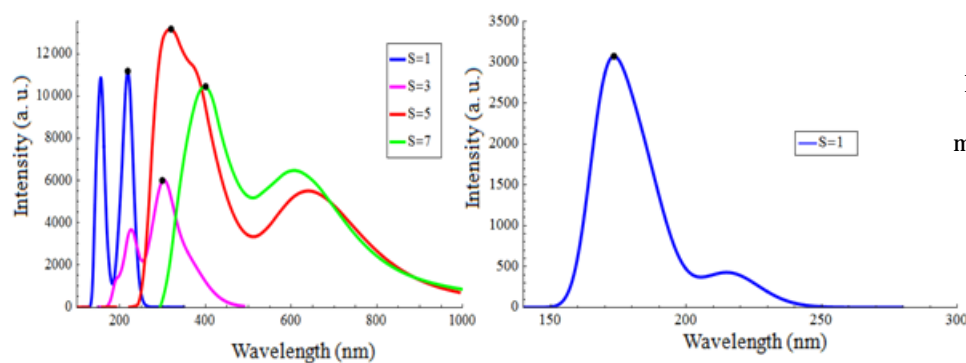


Fig. 7: Theoretical absorption spectra for: neutral HEMA at different spin multiplicity(a); neutral poly(HEMA) with DP=3 (b)

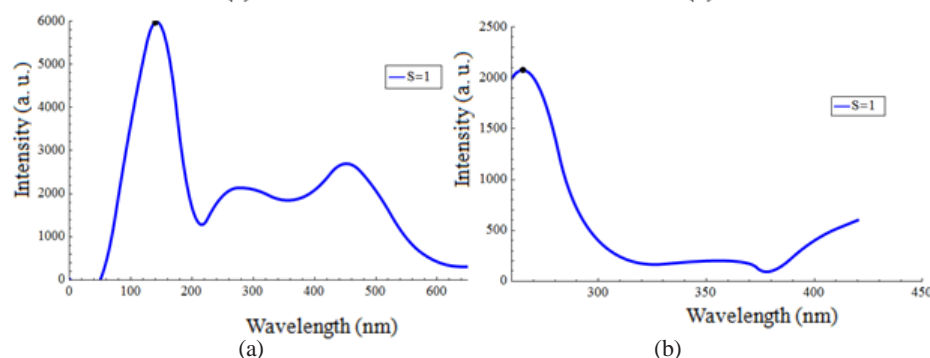


Fig. 8: Theoretical absorption spectra for: (a) neutral HEMA (b) neutral poly(HEMA) with DP=3, with a formal charge +2

Since the spin multiplicity is difficult to determine for complex molecules, the first calculations for neutral HEMA were performed for different allowed values of spin multiplicity:  $S=1$ ,  $S=3$ ,  $S=5$ ,  $S=7$  and the absorption spectra is represented in figure 7.

One first observation is that the absorption peaks shifts from UV-C region (for  $S=1$  - two peaks, very close as intensity, at  $\lambda=150$  and  $\lambda=290$  nm) to VIS (for  $S=7$  -  $\lambda=400$ nm), existing also the possibility to absorb in VIS, but with lower intensity.

For time saving in computational running, next, it was analyzed only the state with spin multiplicity, that in this first running exhibits the entire absorption spectra in UV region.

Poly(HEMA) absorbs, also, in UV, but the absorption peaks decrease as intensity and is more concentrated around  $\lambda=175$  nm, the absorption in VIS being negligible (fig. 7).

#### Spectral properties of HEMA and poly(HEMA) in electrically charged state

When considering Poly(EuHEMA) complexes, the ligand is bonded to lanthanide ion and therefore, we must assign to HEMA and poly(HEMA) a formal charge; its value was evaluated taking into considerations the results from experimental analysis, i.e. the ligand bonds to the lanthanide ions with a covalent bond (by sharing electrons) and a coordinative bond by donating electrons. Therefore, we estimated a formal charge of  $+2$  for the ligand charge and we calculated the excited states for both HEMA and poly(HEMA). The resulted absorption spectra are plotted in figure 8.

As can be seen, in the case of HEMA monomer, the excitation peak was estimated around, in UV region, higher than in the case of isolated HEMA, but, by comparison with the experimental excitation spectra, shape similarities were observed.

By increasing the number of the monomer unit of the poly(HEMA) to 3, the absorption peak was now calculated at 265 nm, closer to the experimental value.

## Conclusions

In this paper, computational calculations were performed in order to obtain information about the electrostatic distribution of electric charges inside polymer, with consequences on the absorption spectra. The results revealed that: (i) the electron density rearrange itself from the main chain to the branch chain and towards one terminal residue of the polymer, suggesting a noninvolvement in chemical reactions of the atoms; (ii) electrically neutral poly(HEMA) exhibits absorption in UV, with absorption peak around , the absorption in VIS being negligible; (iii) poly(HEMA) electrically charged with a formal charge of +2 (assigned due to the coordinative bond established with the lanthanide ion by donating a pair of electrons), a high similarity degree between experimental and theoretical absorption spectra is observed, with a theoretical absorption peak estimated around 265nm, very close to the experimental one. A higher correlation is expected to be obtained for higher polymerization degrees, direction in which the research will be continued.

These results substantiates the fact that the absorption spectra is determined by the ligand type, while the procedure used can be applied for the accurate prediction of absorption spectra for different type of polymeric ligands.

*Acknowledgment: This work was supported by a grant of the Romanian National Authority for Scientific Research and Innovation, CNCS/CCCDI -UEFISCDI, project number PN-III-P2-2.1-PED-2016-0760, 77PED/2017, within PNCDI III.*

## References

1. TEO, R.D., TERMINI, J., GRAY, H.B., J. Med. Chem., **59**, 2016, p. 6012
2. POPESCU, M. R., PLESEA, I. E., OLARU, M., et al., Rom. J. Morphol. Embryol., **56**, 2015, p. 967
3. STIRBU, I., VIZUREANU, P., CIMPOESU, R., POSTOLACHE, P., et. al., J. Optoelectron. Adv. M., **17**, 2015, p. 1179
4. LAUTERBUR, P.C., Nature, **242**, 1973, p. 190
5. LAUFFER, R. B., Chem. Rev., **87**, 1987, p. 901
6. LOUIE, A., Chem. Rev., **110**, 2010, p. 3146
7. HAN, G., DENG, Y., SUN, J., et. al., Exp. Ther. Med., **9**, 2015, p. 1561
8. OPREA, O., STANESCU, M.D., JITARU, I. et. al., Rev. Chim.(Bucharest), **63**, 2012, no. 2, p. 166
9. CONSTANTIN, B., POSTOLACHE, P., CROITORU, A., NEMES, R.M., J. Environ. Prot. Ecol., **16**, 2015, p. 517

10. DOROFTEI, B., MAMBET, C., ZLEI, M., PLoS One, **10**, 2015, e0125216
11. AGOP, M., GAVRILUT, A., STEFAN, G., DOROFTEI, B., Entropy, **17**, 2015, p. 2184
12. CARAC, A., BOSCENCU, R., CARAC, G., BUNGAU, S. G., Rev. Chim. (Bucharest), **68**, no. 10, 2017, p. 2265
13. MARINESCU, G., CULITA, D.C., PATRON, L., et. al., Rev. Chim.(Bucharest), **65**, 2014, p. 426
14. LEIF, R. C., VALLARINO, L. M., BECKER, M. C., YANG, S., Cytometry A, **69**, 2006, p. 767
15. PARKER, D., WILLIAMS, J.A.G., J. Chem. Soc. Dalton Trans., **18**, 1996, p. 3613
16. BINNEMANS, K., Coord. Chem. Rev., **295**, 2015, p. 1
17. AGOP, M., NICA, P., GIRTU, M., Gen. Relativ. Gravit., **40**, 2008, p. 35
18. FREIRE, R.O., ROCHA, G. B., A.M. SIMAS, A. M., Inorg. Chem., **44**, 2005, p. 3299
19. FREIRE, R.O., ROCHA, G. B., A.M. SIMAS, A. M., J. Braz. Chem. Soc., **20**, 2009, p. 1638
20. DUTRA, L., J. D., BISPO, T. D., FREIRE, R. O., J. Comput. Chem., **35**, 2014, p. 772
21. PLATAS-IGLESIAS, C., ROCA-SABIO, A., REGUEIRO-FIGUEROA, M., et. al., Curr. Inorg. Chem., **1**, 2011, p. 91
22. STAN, C. S., PEPTU, C. A., URSU, L.E., HORLESCU, P., J. Inorg. Organomet. Polym. Mater. (under review)
23. HANWELL, M. D., CURTIS, D.E., LONIE, D. C., VANDERMEERSCHD, T., et. al. , J. Cheminf., **4**, 2012, p. 17
24. FRISCH, M. J.; TRUCKS, G. W.; SCHLEGEL, H. B.; SCUSERIA, G. E.; ROBB, M. A.; CHEESEMAN, J. R.; SCALMANI, G.; BARONE, V.; MENNUGGI, B.; PETERSSON, G. A.; NAKATSUJI, H.; CARICATO, M.; LI, X.; HRATCHIAN, H. P.; IZMAYLOV, A. F.; BLOINO, J.; ZHENG, G.; SONNENBERG, J. L.; HADA, M.; EHARA, M.; TOYOTA, K.; FUKUDA, R.; HASEGAWA, J.; ISHIDA, M.; NAKAJIMA, T.; HONDA, Y.; KITAO, O.; NAKAI, H.; VREVEN, T.; MONTGOMERY, J. A., JR.; PERALTA, J. E.; OGLIARO, F.; BEARPARK, M.; HEYD, J. J.; BROTHERS, E.; KUDIN, K. N.; STAROVEROV, V. N.; KEITH, T.; KOBAYASHI, R.; NORMAND, J.; RAGHAVACHARI, K.; RENDELL, A.; BURANT, J. C.; IYENGAR, S. S.; TOMASI, J.; COSSI, M.; REGA, N.; MILLAM, J. M.; KLENE, M.; KNOX, J. E.; CROSS, J. B.; BAKKEN, V.; ADAMO, C.; JARAMILLO, J.; GOMPERS, R.; STRATMANN, R. E.; YAZYEV, O.; AUSTIN, A. J.; CAMMI, R.; POMELLI, C.; OCHTERSKI, J. W.; MARTIN, R. L.; MOROKUMA, K.; ZAKRZEWSKI, V. G.; VOTH, G. A.; SALVADOR, P.; DANNENBERG, J. J.; DAPPRICH, S.; DANIELS, A. D.; FARKAS, O.; FORESMAN, J. B.; ORTIZ, J. V.; CIOŚŁOWSKI, J.; FOX, D. J. Gaussian 09 revision C.01; Gaussian, Inc.: Wallingford, CT, 2010, 2011
25. CASE, D.A., CHEATHAM, T.E., DARDEN, T. H., et. al., J. Computat. Chem. **26**, 2005, p. 1668

Manuscript received: 29.03.2018